Wavenumber Limitation of Medium in the Finite-Difference Modeling of Seismic-Wave Propagation: A Proof of Concept

Jozef Kristek[1,2], Jaroslav Valovcan[1], Peter Moczo[*1,2], Miriam Kristekova[1,2], Rune Mittet[3,4], and Martin Galis[1,2]

Abstract

When developing a finite-difference (FD) scheme, one of the key aspects that must be addressed is the spatial discretization of material parameters and the implementation of material interfaces. Mittet (2017) and Moczo *et al.* (2022) recently suggested a novel approach based on the wavenumber limitation of the medium. They demonstrated that, due to spatial discretization, a model of the medium must be wavenumber-limited by a wavenumber k_m smaller than the Nyquist wavenumber. Mittet (2021a) and Valovcan *et al.* (2024) proved that the wavefield (numerically simulated or exact) in a k_m-limited medium can only be accurate up to $k_m/2$. Here, we numerically demonstrate a perfect subcell resolution (capability to sense the position of interface within a grid cell) of FD modeling based on the wavenumber-limited medium using a finite spatial low-pass filter. The finding that it is possible to use a finite-length filter for wavenumber limitation of the medium is of key importance for the next development of the concept in terms of computational efficiency. We demonstrate an unprecedented accuracy for a canonical model—a material interface between two homogeneous half-spaces. The time–frequency envelope and phase misfits between the FD solution and the exact analytical solution are surprisingly small and are the same for any position of the interface within a grid spacing. We show that the misfits for the reflected and transmitted waves are solely due to grid dispersion. We compare the accuracy of the FD solution for the wavenumber-limited medium with that for the harmonically averaged modulus (Moczo *et al.*, 2002). The FD modeling based on the wavenumber-limited medium is considerably more accurate. The proof of concept of the wavenumber limitation of the medium should be followed by development of a practical way of wavenumber limitation using finite spatial filters in 2D and 3D elastic problems.

Cite this article as Kristek, J., J. Valovcan, P. Moczo, M. Kristekova, R. Mittet, and M. Galis (2025). Wavenumber Limitation of Medium in the Finite-Difference Modeling of Seismic-Wave Propagation: A Proof of Concept, *Seismol. Res. Lett.* **97**, 1965–1975, doi: 10.1785/0220250256.

Introduction

Discretization (sampling) of a continuous signal causes its spectrum to become periodic, introducing potential aliasing, unlike the original continuous spectrum, which is typically nonperiodic and unbounded. This is true for time signals and for functions of spatial coordinates.

The equation of motion and constitutive law include material parameters (e.g., density and elastic moduli) depending on spatial coordinates, and wavefield variables (e.g., particle velocity and stress) that are functions of both spatial coordinates and time.

The finite-difference (FD) method applies relatively simple discretization in space to the material parameters and discretization in space and time to wavefield variables. Therefore, consequences of discretization must be analyzed in the time, space, frequency, and wavenumber domains.

FD schemes for modeling seismic-wave propagation have been developed approximately since the mid-60s of the twentieth century. At that time, the finite-element method dominated. It was just the relatively simple notion of discretization in time and space that motivated seismologists to apply the FD approach to seismic-wave propagation.

The development of the FD schemes has usually been based on necessary analysis of consistency, stability, and subsequently

1. Faculty of Mathematics, Physics and Informatics, Comenius University Bratislava, Bratislava, Slovakia, https://orcid.org/0000-0002-2332-541X (JK); https://orcid.org/0000-0001-5276-9311 (PM); https://orcid.org/0000-0001-9017-5952 (MK); https://orcid.org/0000-0002-5375-7061 (MG); 2. Earth Science Institute, Slovak Academy of Sciences, Bratislava, Slovakia; 3. Allton AS, Stavanger, Norway; 4. RMGS OMS, Trondheim, Norway

*Corresponding author: moczo@fmph.uniba.sk

grid dispersion as a consequence of discretization in time and space. The analysis usually assumed a harmonic plane wave in a homogeneous medium and was performed in the time–space domain. We refer to Moczo *et al.* (2014), Jiang and Zhang (2021), Liu (2022), Koene *et al.* (2022), Zhou *et al.* (2022, 2024), and Chen *et al.* (2024) for a basic overview of the FD method.

Considerably less obvious was how to properly represent material heterogeneity, mainly the internal interface, in the spatial grid. What has been missing was the appropriate account for consequences of the spatial discretization of the medium and wavefield in the wavenumber domain. We refer to Mittet (2017), Mittet (2021a,b), Moczo *et al.* (2022), and Valovcan *et al.* (2023, 2024) for the recent overview of the problem of accuracy of implementation of the material interface and for fundamental insight into accuracy through the wavenumber domain analysis. We do not repeat here the numerous references to relevant contributions present in the articles mentioned. However, we want to especially acknowledge Mora (1986), Holberg (1987), Igel *et al.* (1995), and Fichtner (2011) who pointed out the important aspect of the wavenumber-domain view in replacing spatial derivatives by the wavenumber-limited discrete operators.

In this article, we focus on the possibility to use a finite-length filter in the spatial domain for wavenumber limitation of a heterogeneous medium (bandlimitation of the wavenumber spectrum of a material parameter). For examining accuracy and subcell resolution of an FD solution based on the wavenumber-limited representation of a heterogeneous medium, we use a stringent canonical model of a sharp heterogeneity —a material interface between two homogeneous half-spaces. We compare the FD solution with the exact solution.

Because we are addressing the FD method, we will use the term "grid spacing," here denoted as h, for the sampling step in the spatial domain and "time step" for the sampling step in the time domain. We will briefly cover the well-known aspects and recent surprising findings related to the spatial discretization of the medium and the wavefield.

Introducing Considerations on Wavefields in a Homogeneous Medium

Assume a spatial grid with a grid spacing h. If a function is discretized (sampled) with a grid spacing h, its Fourier wavenumber spectrum is periodic with period

$$2\,\frac{\pi}{h} =: 2k_N(h). \tag{1}$$

The relation defines the Nyquist wavenumber k_N: if the sampling with h should not cause aliasing, the range of the wavenumber spectrum must be limited by

$$k_{\max} \le \frac{\pi}{h} \equiv k_N(h). \tag{2}$$

In other words, a discrete spatial grid with grid spacing h cannot support wavenumbers larger than $k_N(h)$. (Note that here we fix, for a while, the grid spacing h, not k_{max}.)

Assume a source of a wavefield with spectrum limited by ω_{max} and a homogeneous medium with wavespeed c. These two parameters determine the maximum wavenumber k_{max} and the corresponding minimum wavelength λ_{min} of the wavefield:

$$k_{\max} = \frac{\omega_{\max}}{c}, \quad \lambda_{\min} = \frac{2\pi}{k_{\max}}. \tag{3}$$

In other words, in the homogeneous medium, the exact wavefield is wavenumber limited if the source is frequency limited. Assume now a spatial grid with grid spacing h. Relations (2) and (3) imply that the minimum number of grid spacings per λ_{min} must be at least 2:

$$N_{\lambda\,\min} := \frac{\lambda_{\min}}{h} = 2\,\frac{k_N}{k_{\max}} \ge 2. \tag{4}$$

In FD modeling, this criterion is applied to the minimum wavelength, that is in the spatial domain. The criterion usually does not pose a concern in the time domain because the stability of a scheme imposes considerably more severe restriction to values of the time step (discretization in time).

All this has been well known since the beginning of the development of FD schemes. We included this explicit brief explanation just because it is the first step of consideration. The second step may be found to be quite surprising by many.

Phenomenon of Wavefield Accuracy Limit in a Wavenumber-Limited Heterogeneous Medium

We say that a function of spatial coordinates (e.g., a material parameter or wavefield variable) is wavenumber limited if its wavenumber Fourier spectrum is nonzero only up to some finite wavenumber. Otherwise, we say that the function is not wavenumber limited. For example, contrary to the homogeneous medium, a material parameter in the heterogeneous medium might not be wavenumber limited.

Importantly, no matter whether the medium is wavenumber limited or not, the exact wavefield in any heterogeneous medium is not wavenumber limited (see Valovcan *et al.*, 2024).

The spatial grid discretizes (samples) a material parameter as a function of spatial coordinates. The spatial discretization does not remove a potential wavenumber content above the Nyquist wavenumber $k_N(h)$. So, obviously, assuming a grid spacing h, if the wavenumber spectrum of a material parameter is effectively nonzero above $k_N(h)$, the medium must be wavenumber limited by $k_N(h)$ prior to the spatial discretization.

The question is what happens with a wavefield (in principle not wavenumber limited) in the k_N-limited medium. Mittet (2017) was the first to address this fundamental question and

obtained preliminary indications for the answer in his investigation of the interface error. Later, Mittet (2021a) reported that if the discrete grid model of a medium coincides with the true medium up to some wavenumber, the simulated wavefield is accurate only up to half of this wavenumber. Valovcan *et al.* (2024) analyzed the question in relation to both the exact and numerically simulated wavefields.

Here, we briefly outline the exemplary 1D test case presented by Valovcan *et al.* (2024). Consider a model of a thin homogeneous layer between two identical homogeneous half-spaces. We apply a wavenumber bandlimitation to the model with three different values of the limiting wavenumber k_m: $k_m = 2\pi/\lambda_m = \{2\pi,4\pi,10\pi\}\mathrm{m}^{-1}$. (Note that, due to the structure of the governing equations, the wavenumber limitation must be applied to compliance and density.) Thus, there are four models: the exact model and the three wavenumber-limited models. The wavefield in each model is due to a plane-wave incident in the lower half-space and propagating upward to the thin layer and the upper half-space. Let f_m be the frequencies of the wavefield corresponding to k_m.

For each model we used the matrix (i.e., exact) method. We approximated the wavenumber-limited models by the stack of thin layers and checked that further reduction of the layer thickness does not change the result in the considered frequency range. We calculated the wave transmitted from the lower half-space through the thin layer into the upper half-space and the wave reflected at the thin layer back to the lower half-space.

The transmitted wave in each wavenumber-limited model is the same as the transmitted wave in the exact model in the entire frequency range, that is, in the entire corresponding range of wavenumbers.

Results for the reflected waves may be considered surprising. Systematically, the reflected wave in each wavenumber-limited model exists and is the same as the reflected wave in the exact model only up to frequency $f_m/2$, that is, only up to wavenumber $k_m/2$.

For the model of two half-spaces, the result is the same except that the reflected wave exists also beyond $f_m/2$ or $k_m/2$. Beyond this limit, the reflected wave is, however, very different from the exact wave in the exact model.

We emphasize that we speak about exact wavefields, not wavefields obtained by a numerical method.

Consequence of Wavefield Accuracy Limit for the FD Modeling

The phenomenon of wavefield accuracy limit in a wavenumber-limited medium has a serious consequence for the FD modeling. If we want the wavefield to be accurate up to wavenumber $k_{\max}$, we must limit the model of the medium by wavenumber $k_m = 2k_{\max}$. What does it mean for the choice of grid spacing? If grid spacing h is needed for fulfilling condition $k_{\max} \le k_N(h)$, then it is obvious that twice the smaller grid spacing $h/2$ is needed for fulfilling condition $k_{\max} \le 2k_N(h) = k_N(h/2)$.

Practically taken: no matter which FD scheme we use, if we want the wavefield to be accurate up to wavenumber $k_{\max} = 2\ \pi/\lambda_{\min}$, we must

1. choose such grid spacing h that $h \le \lambda_{\min}/4$,
2. wavenumber limit the medium by $2k_{\max}$, and
3. discretize (sample) the wavenumber-limited medium using the grid spacing h.

It seems to us that it is not easy to intuitively understand this relation between the wavenumber limitation of the medium and wavenumber limitation of the wavefield. Valovcan *et al.* (2024) provided an explanation based on the application of the Lippmann–Schwinger equation in the Born approximation of the first order for scattered wavefields.

How to Wavenumber Limit the Medium?

If we know that, given a spatial grid, the medium must be correspondingly wavenumber limited, let us look at the wavenumber limitation itself.

An ideal filter for the k_m limitation of the material parameter $M(z)$ for a scheme without grid dispersion would be

$$\tilde{F}(k) = \begin{cases} 1; & 0 \le k \le k_m \\ 0; & k_m < k \end{cases}, \tag{5}$$

in which k_m would be equal to a corner wavenumber k_{cor} and a cutoff wavenumber k_{cut},

$$k_m = k_{\mathrm{cor}} = k_{\mathrm{cut}}, \tag{6}$$

as illustrated in Figure 1a.

The problem is that the ideal filter is not applicable because the corresponding wavenumber-limited medium would have an infinite spatial extent with nonnegligible variations of the value of the material parameter over relatively large spatial extent. What "relatively" means may depend on the model heterogeneity, size of the computational region, the source, and extent of an FD stencil.

Therefore, we must use a filter with $k_{\mathrm{cor}} < k_{\mathrm{cut}}$. The value of k_{cor} must be larger than or equal to k_m, and k_{cut} must be smaller than or equal to k_N. The best possibility would be $k_{\mathrm{cor}} = k_m = 2k_{\max}$, that is, k_{cor} would correspond to $h = \lambda_{\min}/4$. The filter is illustrated in Figure 1b.

The choice of k_{cut} has several aspects to be considered. Depending on the FD scheme, more than four grid spacings per $\lambda_{\min}$ might be required due to grid dispersion. The minimum wavespeed in the wavenumber-limited medium may be smaller than $c_{\min}$ due to oscillatory character of the wavenumber-limited medium. Because of these two aspects, k_{cut} should be sufficiently larger than $k_{\mathrm{cor}} = k_m$. Therefore, instead of the grid spacing $h = \lambda_{\min}/4$ we should use a grid spacing

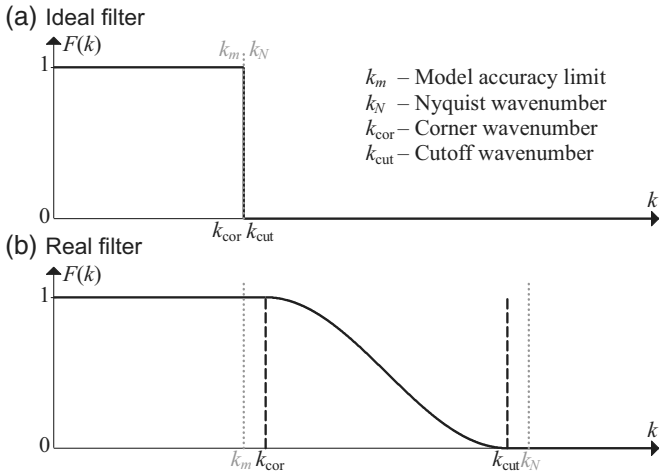

Figure 1. (a) An ideal wavenumber filter for k_m limitation of a material parameter. (b) Real filter.

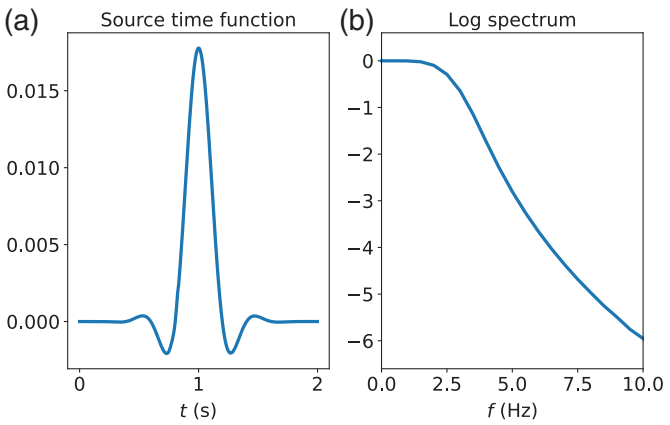

Figure 2. (a) Source time function and its (b) amplitude Fourier spectrum.

$$h_{\text{cut}} = \frac{k_{\text{cor}}}{k_{\text{cut}}} h = \frac{k_{\text{cor}}}{k_{\text{cut}}} \frac{1}{4} \frac{c_{\min}}{f_{\max}}. \tag{7}$$

Obviously, the values of k_{cut} and k_{cor} determine the spatial extent of the nonnegligible variations of the wavenumber-limited medium.

As already mentioned, in practice, that is in numerical simulations, the spatial extent is limited by the material heterogeneity, the finite grid, the free surface, and possibly also by the source. The corresponding limitations for the spatial extent of the wavenumber-limited medium could potentially cause values of k_{cut} larger than those required by the grid dispersion of the FD scheme. Therefore, it is necessary to make an approximation as a compromise in the presence of several factors affecting accuracy of the modeling. The compromise mainly relates to the wavenumber filter.

Denoting a material parameter by P and filter by F, we recall the relation

$$\mathcal{F}^{-1}_{k\to z}\{\tilde{F}(k)\ \tilde{P}(k)\} = F(z) * P(z). \tag{8}$$

We see that in practice it might be reasonable to (1) design a filter in the wavenumber domain, (2) transform it to the spatial domain with sampling considerably finer than the grid spacing, (3) restrict its spatial extent using a suitable window, (4) check the spatially restricted filter in the wavenumber domain, and, if acceptable, (5) apply the filter in the spatial domain through the convolution with the material parameter, and (6) downsample the material parameter.

Numerical Test: Accuracy of a Reflected Wave

Configuration

Consider a 1D problem for a model of two homogeneous half-spaces. The wavespeeds in the lower and upper half-spaces are 300 and 100 m/s, respectively. A constant density of 2500 kg/m^3 is assumed. A plane wave is generated 600 m beneath the interface. The source time function is obtained by application of the Butterworth filter to the Fourier spectrum of the Dirac impulse and a subsequent application of the Blackman window in the time domain. The source time function and its amplitude Fourier spectrum are shown in Figure 2. The spectral amplitude falls by three orders approximately at the frequency of 5 Hz. Therefore, we will consider this frequency as a reasonable maximum frequency of the wavefield. The corresponding minimum wavelength is $\lambda_{min} = 100$ m/s/5 Hz $= 20$ m, and the corresponding maximum wavenumber is $k_{\max} = 2\pi/\lambda_{\min} = \pi/10$ m^{-1}.

The plane wave propagates upward in the lower half-space and reaches the interface. A transmitted wave propagates upward in the upper half-space, and a reflected wave propagates downward in the lower half-space. As explained in the exemplary 1D test presented by Valovcan *et al.* (2024), we should be primarily interested in the reflected wave. We "record" the reflected wave at the position where the plane wave was generated.

For the considered medium-wavefield configuration, we compare three independent solutions for the reflected wave:

- ES is an exact analytical solution.
- FDA is an FD method (staggered-grid, velocity–stress, fourth order in space, second order in time) with arithmetically averaged compliance, that is, harmonically averaged elastic modulus (Moczo *et al.*, 2002, 2014). We use 10 grid spacings per λ_{min}. (This choice is "cautious," ensuring sufficiently small grid-dispersion error without conflicting with the goal of the test.) This means grid spacing $h = 2$ m. Consequently, $k_N = \pi/2$ m^{-1}.
- FDWL is an FD method (staggered-grid, velocity–stress, fourth order in space, second order in time) with a wavenumber-limited medium. If we want to have the wavefield

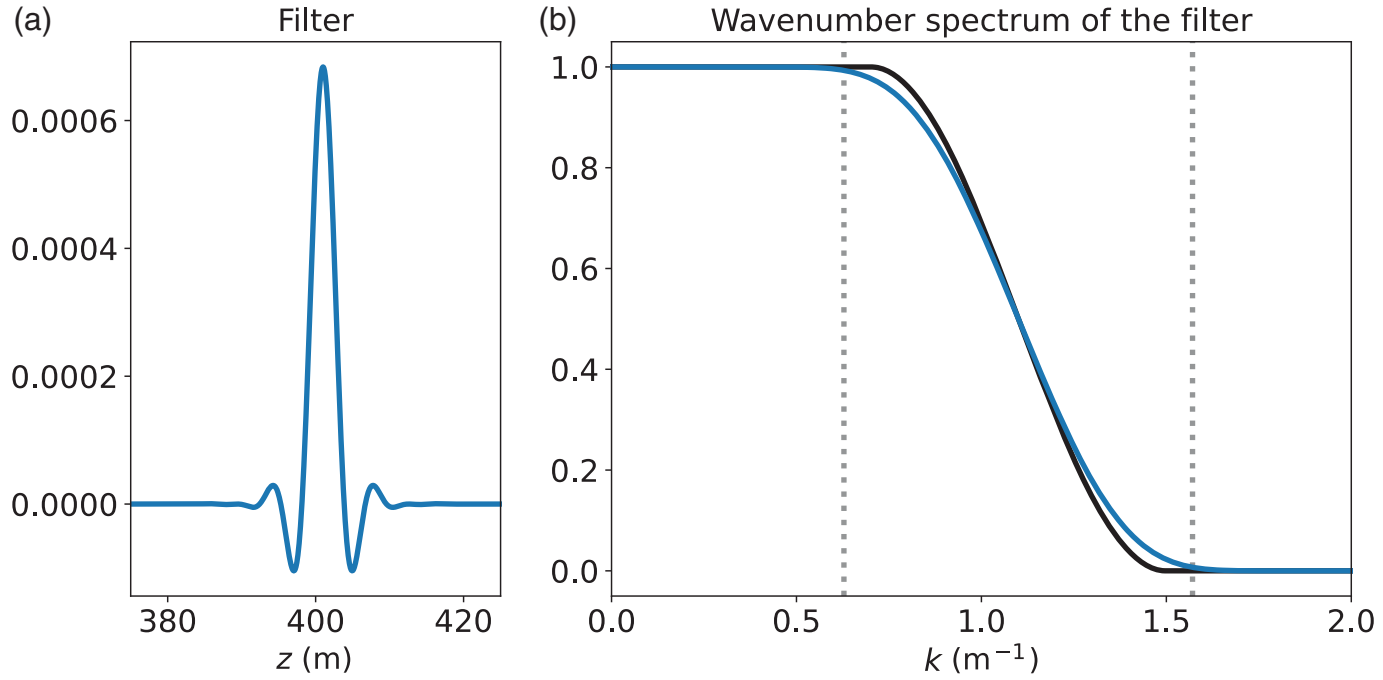

Figure 3. (a) Final spatial filter used for the wavenumber limitation of the medium. (b) Solid black—originally designed filter (as in Fig. 1b), which has an infinite spatial extent. Solid blue—the final (truncated) filter corresponding to the spatial filter in panel (a). The left-vertical dotted bar corresponds to the wavenumber accuracy limit k_m. The right-vertical dotted bar corresponds to the Nyquist wavenumber k_N.

sufficiently accurate up to wavenumber $k_{\max} = \pi/10$ m^{-1}, we must limit the medium by $k_m = 2k_{\max} = \pi/5$ m^{-1}.

Wavenumber limitation using a spatial filter

For the wavenumber limitation of the medium, we first designed a filter in the wavenumber domain:

$$\tilde{F}(k) = \begin{cases} 1 & k \in [0, k_{\text{cor}}] \\ \frac{1}{2}\left[1 + \cos\left(\pi \frac{k - k_{\text{cor}}}{k_{\text{cut}} - k_{\text{cor}}}\right)\right] & k \in [k_{\text{cor}}, k_{\text{cut}}] \\ 0 & k \geq k_{\text{cut}} \end{cases}. \quad (9)$$

Values of k_{cor} (which must be larger than k_m) and k_{cut} (which must be smaller than k_N) used for the numerical test were, 0.7 and 1.5 m^{-1}, respectively.

The corresponding filter in the spatial domain was obtained by the inverse Fourier transform. Because it has an infinite spatial extent, it must be truncated. We truncated it using the Blackman window

$$W_B = \begin{cases} 0.42 - 0.50\cos\left(\pi \frac{z - z_c + w}{w}\right) + 0.08\cos\left(2\pi \frac{z - z_c + w}{w}\right); |z - z_c| \leq w \\ 0; |z - z_c| > w \end{cases}. \quad (10)$$

The filter is truncated at its zero values at half-width w from its center at z_c. Expertly, we chose $w \approx 12.5h$. The final filter in the spatial and wavenumber domain is shown in Figure 3. As can be seen in Figure 3b, the truncation in the spatial domain slightly modifies the filter in the wavenumber domain. Still, however, for $k < k_m$ it is $\tilde{F}(k) \approx 1$, and for $k > k_{\text{cut}}$ it is $\tilde{F}(k) \approx 0$.

The wavenumber limitation itself is performed by a convolution of the spatial filter with the original compliance.

FDA and FDWL solutions

Assuming the fixed position of the source, each ES, FDA, and FDWL solution corresponds to a specific position of the true interface in a spatial FD grid. This is because both FDA and FDWL approaches make it possible to consider an arbitrary position of the interface within a grid spacing (in 1D this means anywhere within one grid cell).

In the FDA approach, we account for a position of the interface within a grid spacing by evaluating effective grid modulus at grid position (here, e.g., $I + 1/2$) as an integral harmonic average between grid points I and $I + 1$ (Moczo *et al.*, 2002, 2014)

$$M^H_{I+1/2} \equiv \left[\frac{1}{h}\int_{z_I}^{z_{I+1}} \frac{1}{M(z)}\,\mathrm{d}z\right]^{-1}. \quad (11)$$

The harmonic averaging of the modulus is equivalent to arithmetic averaging of the compliance. Moczo *et al.* (2002, 2014) demonstrated a very good level of accuracy and very good subcell resolution of this representation of the material interface.

In the FDWL approach, we apply wavenumber limitation to compliance. Then, we calculate the corresponding modulus. Although we did not apply the limitation to the modulus itself, we call it the wavenumber-limited modulus. Then we simply position, say $M^{\text{WL}}_{I+1/2}$, in the grid points. In Figure 4, we show

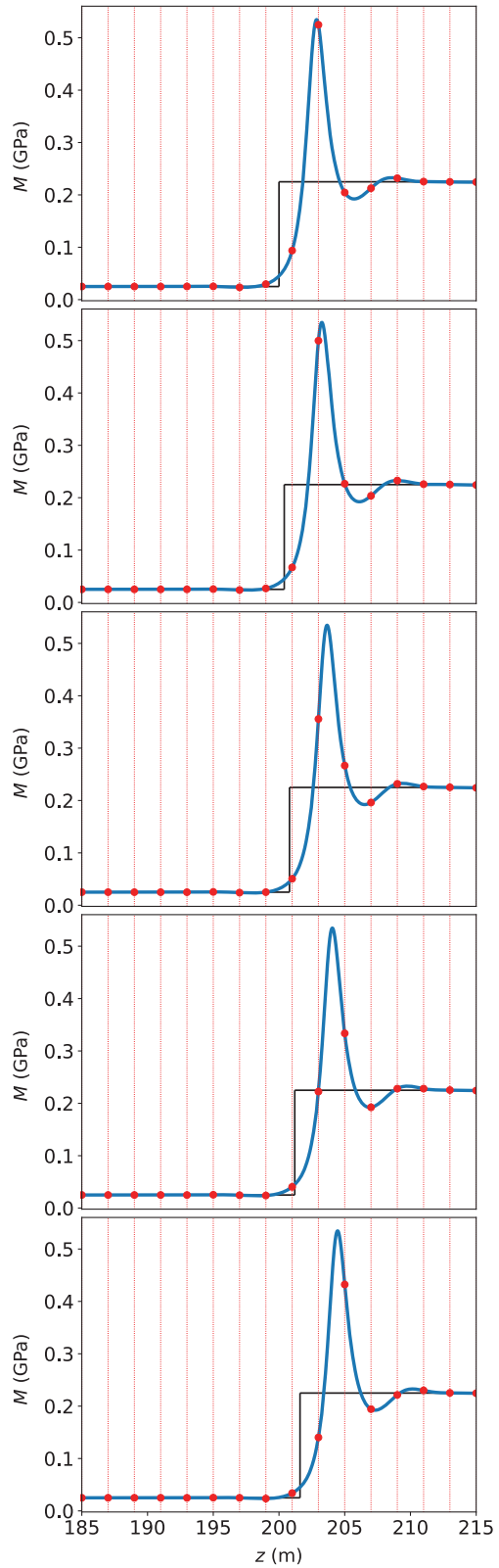

Figure 4. Five positions of the material interface in the spatial grid used for finite-difference (FD) simulations. The true modulus $M(z)$ is shown in solid black. Red-dotted lines represent grid lines (in 1D representing grid positions of stress). Solid-blue line represents the wavenumber limited modulus $M^{\mathrm{WL}}(z)$, and red dots represent values of $M^{\mathrm{WL}}_{I+1/2}$ entering the FD scheme for the FDWL simulation.

five different positions of the interface within a grid spacing. In each of the five panels, the red-dotted lines represent grid lines (in 1D representing grid points—positions of stress and thus also modulus in the staggered grid). The true modulus $M(z)$ is shown in solid black, and the wavenumber-limited modulus $M^{\mathrm{WL}}(z)$ is shown in solid blue. Red dots represent values of $M^{\mathrm{WL}}(z)$ sampled by the spatial grid, that is, $M^{\mathrm{WL}}_{I+1/2}$ values. Note that just these sampled values represent the wavenumber-limited medium in the FD scheme.

We can clearly see that each position of the true interface in the grid (shown in solid black) is represented in the wavenumber-limited medium by differently positioned samples (red dots) of $M^{\mathrm{WL}}(z)$. Note that only in two positions of the interface is $M^{\mathrm{WL}}(z)$ sampled close to its peak value.

Comparison of FDA and FDWL with the exact solution

We removed the incident wave from the total wavefield in the lower half-space to obtain the reflected wave. We compare reflected waves in the three solutions, that is, exact, FDA, and FDWL, in Figure 5 using time–frequency envelope misfit (TFEM) and time–frequency phase misfit (TFPM) according to Kristekova *et al.* (2009). The figure consists of five panels. Each panel compares three solutions for one of the five positions of the material interface in the grid shown in Figure 4. The position is indicated in the left column. The left of the comparing panels shows TFEM and TFPM between the FDA and the exact solutions. The right panel shows TFEM and TFPM between the FDWL and the exact solutions. Signal of the reflected wave is also shown for all three solutions. The values of the single-valued envelope misfit (EM) and phase misfit (PM) evaluated over the entire time and frequency ranges are also shown.

There are two most striking features of the comparison: (a) TFEM and TFPM between the FDWL and exact solutions do not change with the position of the interface in the grid, and the maximum EM and PM are as low as 0.08% and 0.07%, respectively; (b) TFEM and TFPM between the FDA and exact solution vary, but they are all smaller than or equal to 0.38% and 0.09%, respectively. This is why we cannot recognize FD seismograms from the exact seismograms and see only one (red) color of the seismogram. In other words, both FD solutions are excellent and with subcell resolution, but FDWL is simply better because its accuracy does not change with the position of the interface in the grid.

The accuracy of the FDWL solution for any position of the interface in the grid can be demonstrated also in Figure 6. Again, we compare FDA versus the exact solution and FDWL versus the exact solution. Here, we show only time envelope misfit, however, for 13 positions within a grid spacing. All misfits between the FDA and the exact solution are shown in the left frame. We can see that misfits for different positions of the interface differ from each other. At the same time, they are all very small—the absolute values are less than 0.5%. The

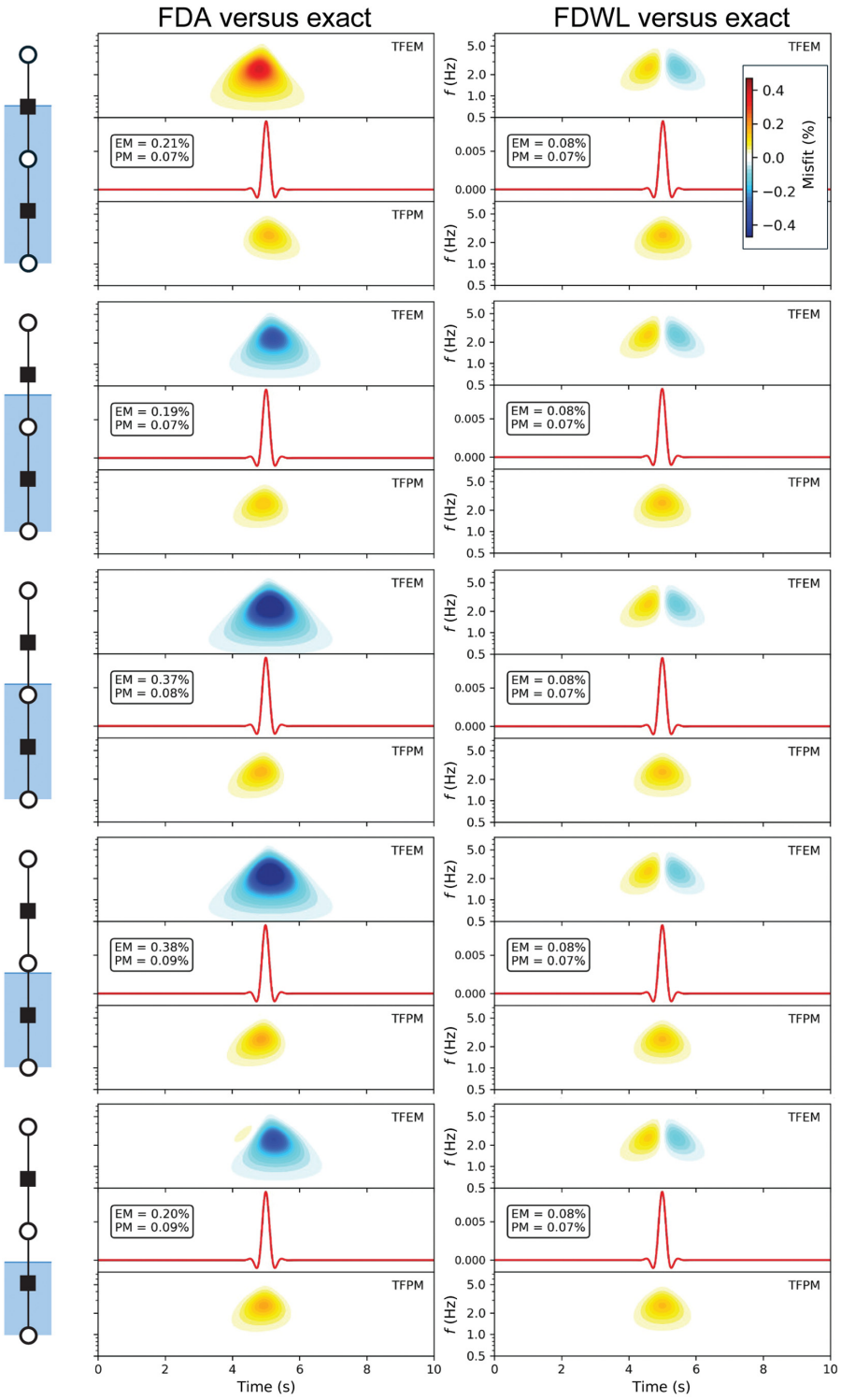

Figure 5. Comparison of the FDA (FD with arithmetically averaged compliance—corresponding to the harmonically averaged modulus) and FDWL (FD with wavenumber-limited compliance) solutions with the exact analytical solution using time–frequency envelope misfit (TFEM) and time–frequency phase misfit (TFPM) for the wave reflected from the interface between two half-spaces. The left column shows positions of the material interface in the FD spatially staggered grid. Circles represent grid positions of the stress; black squares represent grid positions of the particle velocity. Signals of the reflected waves are also shown. The exact solution is in solid red, the FD solutions in solid black (not seen due to very good agreement between signals). Single-valued envelope misfit (EM) and phase misfit (PM) evaluated over the entire time and frequency ranges are also shown.

comparison between FDWL and the exact solution confirms what we could see already in Figure 5—the misfit is the same for all positions of the interface in the grid.

In Figure 6, we also show the misfits between the FD solutions and the exact solution for the direct wave. By the direct wave, we mean the wave propagating in the homogeneous medium with material properties of the lower half-space, and propagating the same time as is the time between the radiation of the wave and recording the reflected wave at the receiver. (The same time in the same medium is important to have the same cumulative effect of the grid dispersion.) We can see that the misfit for the direct wave is the same as the misfit for the reflected waves (plural because we consider reflected waves simulated using FDWL for 13 positions of the interface in the grid). This means that there is no interface error in the FDWL solutions and the misfit quantifies nothing else than the grid-dispersion error! The absence of the interface error in all FDWL solutions is a very significant result. The meaning of this result is nothing less than the proof of concept of the wavenumber-limited representation of the material heterogeneity!

Numerical Test: Accuracy Across the Entire Model

In the first numerical test, we looked at the accuracy of the reflected wave at a distance from the interface, which is considerably larger than the extent of the spatial filter used for the wavenumber limitation.

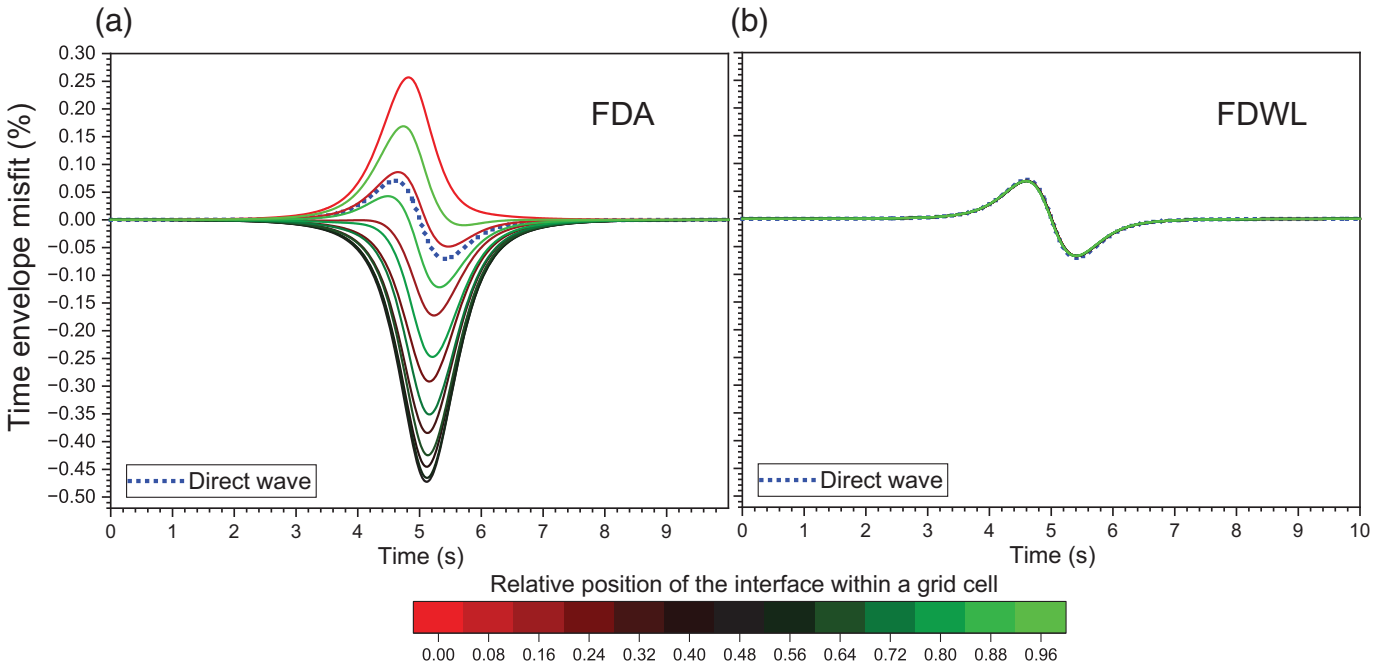

Figure 6. Comparison of (a) FDA (FD with harmonically averaged modulus) and (b) FDWL (FD with wavenumber-limited medium) solutions with the exact analytical solution using time envelope misfit for the wave reflected from the interface between two half-spaces (solid lines with color corresponding to the position of the interface in the grid) and for the direct wave (blue-dotted line). Thirteen positions of the material interface within a grid spacing are considered.

Here, we will look at the accuracy of the wavefield across the entire model. Therefore, we will include also the transmitted wave in the upper half-space.

Configuration and methods of computation

The wavefield-medium configuration is the same as that in the first numerical test. We applied the same three methods to compute the total wavefield. In the upper half-space we obviously obtained the transmitted wave, whereas in the lower half-space we removed the incident wave from the total wavefield to obtain the reflected wave.

Comparison of FDA and FDWL with the exact solution

We compare the three solutions, exact, FDA, and FDWL, using single-valued EM and PM according to Kristekova *et al.* (2009). Figure 7 shows EM and PM between the FD and exact solutions. FDA indicates the EM and PM between FDA and ES. FDWL indicates the EM and PM between FDWL and ES. Both EM and PM are shown as functions of the absolute position of receiver with respect to the interface and the relative position of the interface within a grid spacing. Position 0 m of the receiver (on the vertical axis) corresponds to the top of the grid cell within which we position the interface. Relative position 0.0 of the interface (on the horizontal axis) means the interface at the grid position of the particle velocity (see the top panel in Fig. 5). Relative position 1.0 means the interface just one grid spacing lower—again at the grid position of the particle velocity. For example, point [0.4, 200] means that the receiver is at $z = 200$ m and the interface is at $z = 0.4\ h = 0.8$ m, which means that the receiver is 199.2 m below the interface.

We can easily see several striking features. The two most important at first sight are the principal difference between FDA and FDWL, and the small values of both EM and PM for both FD solutions.

The largest values of PM are restricted to a thin effective layer around the interface in both FD solutions. In the FDA solution, they are smaller than 0.5%, and the thickness of the effective layer is determined by the spatial extent of the FD stencil. In the FDWL solution, they are smaller than 2%, and the thickness of the layer is determined by both the spatial extents of the FD stencil and the filter. Outside the effective layers, PM for both FD solutions is very small.

The largest values of EM are restricted to a thin layer around the interface in the FDWL solution, for which they are smaller than 0.75%. As in the case of PM, the thickness of the layer is determined by both the spatial extents of the FD stencil and the filter. Outside the layer, the extremely small values of EM are caused solely by the grid dispersion (recall Fig. 6). It is very clear that we do not see any dependence of EM or PM on the relative position of the interface within a grid spacing. We should not hesitate to speak about the perfect subcell resolution of the FDWL solution.

In the case of FDA, the largest value of EM is about 0.4% in the lower half-space with higher wavespeed and about 0.15 % in the upper half-space. The largest values are not restricted only to the vicinity of the interface. The amplitude of EM changes only

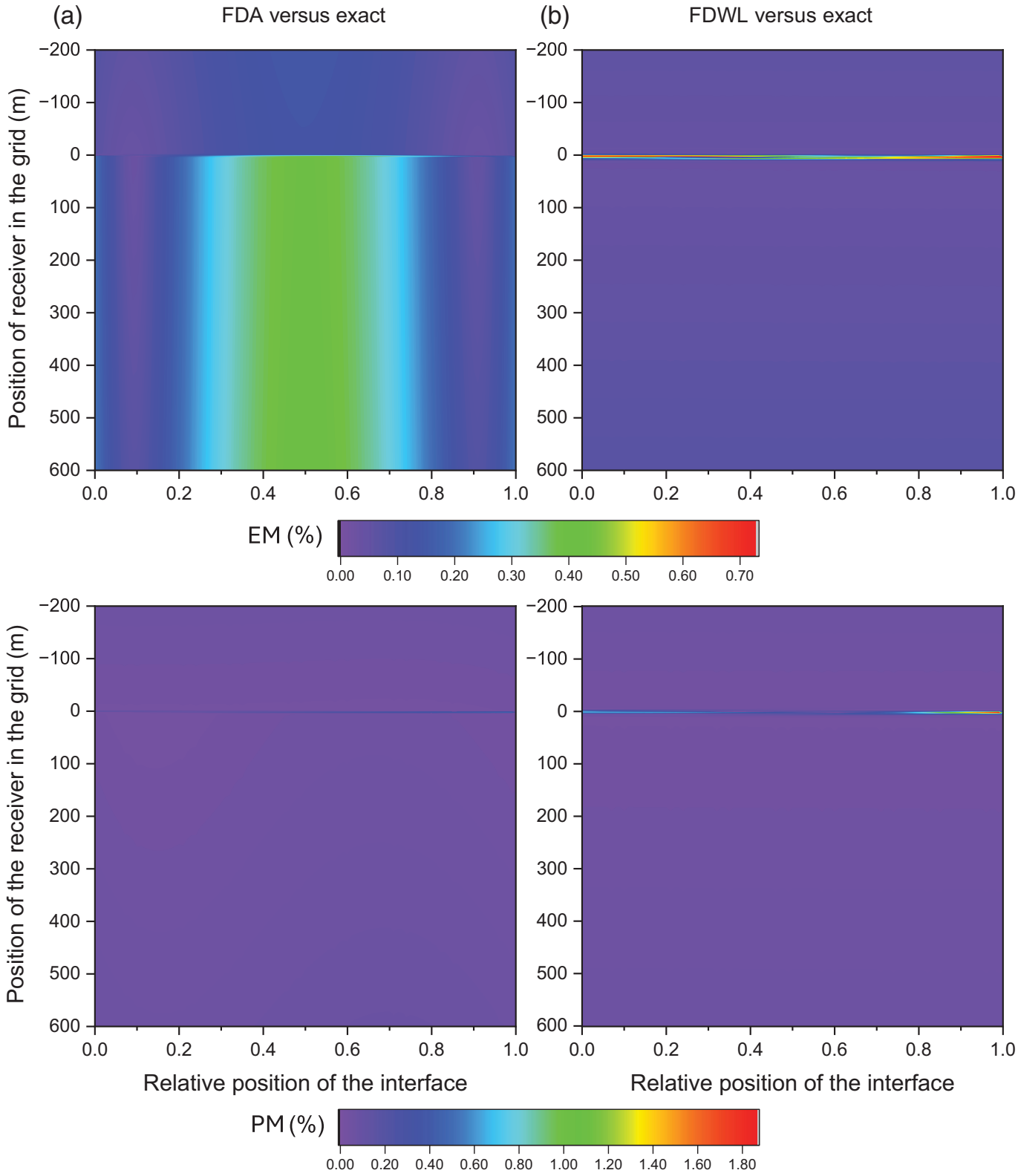

Figure 7. Comparison of (a) FDA and (b) FDWL versus the exact solution for the model of two homogeneous half-spaces. The differences between FD and the exact solutions are quantified by single-valued time-frequency envelope misfit (EM) and single-valued time-frequency phase misfit (PM). The misfit values are overall very small. The principal difference between the FDA and FDWL solutions is that the accuracy of the FDWL solution does not depend on the relative position of the interface within a grid spacing—we may speak of the perfect subcell resolution of the FDWL solution. The misfits of the FDWL solution in the half-spaces are only due to grid dispersion—not affected by the interface error.

slightly with the distance from the interface due to grid dispersion. However, EM varies with the relative position of the interface within a grid spacing. Recall that this variation does not exist in FDWL solution.

EM of both the transmitted and reflected waves in FDA is related to the spatial extent of the fourth-order operator. We checked this by evaluating also EM and PM for the FDA wavefield obtained using a second-order FD scheme. EM and PM are smaller in the second-order solution. This is related to the fact that the harmonic averaging of modulus (Moczo *et al.*, 2002) is applied over one grid spacing and thus is more suitable for the second-order scheme (using an operator with a shorter stencil). Obviously, such an approach requires finer spatial sampling.

Conclusions

This study is a necessary logical continuation, literally a proof of concept, of our current investigations on the accuracy of FD schemes based on the analysis in the wavenumber domain. We have performed a detailed numerical analysis of the accuracy of the implementation of a material interface in FD modeling, following the recently identified limit of accuracy of a wavefield in a wavenumber-limited model of the medium.

For methodological clarity and clean isolation of the effect of wavenumber limitation of the medium, we investigated the accuracy of the reflected and the transmitted waves in a 1D problem of two homogeneous half-spaces. We calculated the wavefield using three methods: exact analytical method, FD scheme (FDA) for arithmetically averaged compliance (i.e., harmonically averaged modulus) and FD scheme (FDWL) for wavenumber-limited medium.

We used a finite-extent spatial filter to wavenumber limit the medium. We evaluated the TFEMs and TFPMs between the FDA and the exact solution as well as the misfits between the FDWL and the exact solution in the entire computational domain. The results of the analysis may be formulated as follows.

1. The time–frequency misfits between the FD and the exact analytical solutions are very small.
2. Both FDA and FDWL have the subcell resolution capability—they can sense different positions of the interface within a grid spacing.
3. However, there is a principal difference between FDA and FDWL. Whereas the subcell resolution of the FDA is not perfect (the misfit between the FDA and the exact solution varies a little bit with position of the interface within a grid spacing), the misfit between the FDWL and the exact solution is the same and very small for any position of the interface within a grid spacing. The misfits in FDWL for the reflected and transmitted waves are solely caused by the grid dispersion of the FD scheme. In other words: FDWL exhibits a perfect subcell resolution, and the demonstrated nature and level of accuracy may be considered proof of concept of the wavenumber limitation of the medium.
4. The largest values of the EM are restricted to a thin layer around the interface in the FDWL solution, for which they are smaller than 0.75%. The thickness of the layer is determined by the spatial extents of the FD stencil and the filter. The most important is the fact that in FDWL, the error at, and very near, the interface does not propagate into half-spaces.

The main conclusion

We have numerically demonstrated accuracy of the implementation of a material interface in FD modeling based on the wavenumber limitation of the medium. We used a finite-extent spatial filter to wavenumber limit the medium. The FD scheme for the wavenumber-limited medium has a perfect subcell resolution: the misfit between the FD and exact solutions is very small and the same for any position of the interface within a grid spacing. The misfits for the reflected and transmitted waves are solely due to grid dispersion. FD modeling for the wavenumber-limited medium is considerably more accurate than that for the harmonically averaged modulus.

It was necessary to provide a detailed numerical proof of concept of the wavenumber-limited medium in the fundamental methodological model—a material interface between the two homogeneous half-spaces. The next step will be to develop finite-extent spatial filtering to wavenumber limit the medium in 2D and 3D. We assume that development of a practical "recipe" will be a challenging task. If successfully developed, we assume that the spatial filtering in 2D and 3D will be applicable also in other most important numerical-modeling methods—spectral-element method (e.g., Komatitsch and Vilotte, 1998; Lyu *et al.*, 2020), discontinuous Galerkin method (e.g., Käser and Dumbser, 2006; Wolf *et al.*, 2020), and the recent and promising distributional FD method (e.g., Masson, 2023; Lyu *et al.*, 2024)—inside an element in which material parameters are functions of spatial coordinates.

Data and Resources

There are no new data or resources to report for this article.

Declaration of Competing Interests

The authors acknowledge that there are no conflicts of interest recoded.

Acknowledgments

The authors thank reviewers Wei Zhang and Chao Lyu for their reviews, which helped them to improve the article. This work was supported by the Slovak Research and Development Agency under the Contract Number APVV-24-0311 (Project SANEFF).

References

Chen, H., K. Chen, L. Wang, H. Zhou, H. Zhang, and W. Sun (2024). An efficient immersed free surface boundary method for 3-D

scalar seismic waves finite-difference modeling in presence of topography, *IEEE Trans. Geosci. Remote Sens.* **62,** 1–12.

Fichtner, A. (2011). *Full Seismic Waveform Modelling and Inversion*, Springer, Heidelberg, Germany.

Holberg, O. (1987). Computational aspects of the choice of operator and sampling interval for numerical differentiation in large-scale simulation of wave phenomena, *Geophys. Prospect.* **37,** no. 6, 629–655.

Igel, H., P. Mora, and B. Riollet (1995). Anisotropic wave propagation through finite-difference grids, *Geophysics* **60,** no. 4, 1203–1216.

Jiang, L., and W. Zhang (2021). TTI equivalent medium parametrization method for the seismic waveform modelling of heterogeneous media with coarse grids, *Geophys. J. Int.* **227,** 2016–2043.

Käser, M., and M. Dumbser (2006). An arbitrary high-order discontinuous Galerkin method for elastic waves on unstructured meshes – I. The two-dimensional isotropic case with external source terms, *Geophys. J. Int.* **166,** 855–877.

Koene, E. F. M., J. Wittsten, and J. O. A. Robertsson (2022). Finite-difference modelling of 2-D wave propagation in the vicinity of dipping interfaces: A comparison of anti-aliasing and equivalent medium approaches, *Geophys. J. Int.* **229,** 70–96.

Komatitsch, D., and J.-P. Vilotte (1998). The spectral element method: An efficient tool to simulate the seismic response of 2D and 3D geological structures, *Bull. Seismol. Soc. Am.* **88,** 368–392.

Kristekova, M., J. Kristek, and P. Moczo (2009). Time-frequency misfit and goodness-of-fit criteria for quantitative comparison of time signals, *Geophys. J. Int.* **178,** 813–825.

Liu, Y. (2022). Removing the stability limit of the time-space domain explicit finite-difference schemes for acoustic modeling with stability condition-based spatial operators, *Geophysics* **87,** no. 3, T205–T223.

Lyu, C., Y. Capdeville, and L. Zhao (2020). Efficiency of the spectral element method with very high polynomial degree to solve the elastic wave equation, *Geophysics* **85,** no. 2, T33–T43.

Lyu, C., Y. Masson, B. Romanowicz, and L. Zhao (2024). Introduction to the distributional finite difference method for 3D seismic wave propagation and comparison with the spectral element method, *J. Geophys. Res.* **129,** no. 4, e2023JB027576, doi: 10.1029/2023JB027576.

Masson, Y. (2023). Distributional finite-difference modelling of seismic waves, *Geophys. J. Int.* **233,** 264–296.

Mittet, R. (2017). On the internal interfaces in finite-difference schemes, *Geophysics* **82,** no. 4, T159–T182.

Mittet, R. (2021a). On the pseudospectral method and spectral accuracy, *Geophysics* **86,** no. 3, T127–T142.

Mittet, R. (2021b). Small-scale medium variations with high-order finite-difference and pseudospectral schemes, *Geophysics* **86,** no. 5, T387–T399.

Moczo, P., J. Kristek, and M. Galis (2014). *The Finite-Difference Modelling of Earthquake Motions: Waves and Ruptures*, Cambridge University Press, Cambridge, United Kingdom.

Moczo, P., J. Kristek, M. Kristekova, J. Valovcan, M. Galis, and D. Gregor (2022). Material interface in the finite-difference modeling: A fundamental view, *Bull. Seismol. Soc. Am.* **113,** no. 1, 281–296.

Moczo, P., J. Kristek, V. Vavryčuk, R. J. Archuleta, and L. Halada (2002). 3D heterogeneous staggered-grid finite-difference modeling of seismic motion with volume harmonic and arithmetic averaging of elastic moduli and densities, *Bull. Seismol. Soc. Am.* **92,** no. 8, 3042–3066.

Mora, P. (1986). Elastic finite differences with convolutional operators, *Stanford Explor. Proj. Rep.* **48,** 277–289.

Valovcan, J., P. Moczo, J. Kristek, M. Galis, and M. Kristekova (2023). Can higher-order finite-difference operators be applied across a material interface? *Bull. Seismol. Soc. Am.* **113,** no. 5, 1924–1937.

Valovcan, J., P. Moczo, J. Kristek, M. Galis, and M. Kristekova (2024). How accurate numerical simulation of seismic waves in a heterogeneous medium can be? *Bull. Seismol. Soc. Am.* **114,** no. 5, 2287–2309.

Wolf, S., A.-A. Gabriel, M. Bader (2020). Optimisation and local time stepping of an ADER-DG scheme for fully anisotropic wave propagation in complex geometries, in *Computational Science – ICCS 2020*, V. V. Krzhizhanovskaya, *et al.* (Editors), Lecture Notes in Computer Science, Vol. 12,139, Springer, Cham, Switzerland.

Zhou, H., Y. Liu, and J. Wang (2022). Elastic wave modeling with high-order temporal and spatial accuracies by a selectively modified and linearly optimized staggered-grid finite-difference scheme, *IEEE Trans. Geosci. Remote Sens.* **60,** 1–22.

Zhou, H., L. Zhang, and Y. Zhang (2024). Simulation of scalar wave propagation with high-order temporal and spatial accuracy by a new multi-axial staggered-grid finite-difference scheme, *Bull. Seismol. Soc. Am.* **115,** no. 1, 1–21.

Manuscript received 4 August 2025
Published online 9 December 2025